11th Australasian Fluid Mechanics Conference
University of Tasmania, Hobart, Australia
14-18 December 1992

THE STABILITY OF SPATIALLY DEVELOPED PIPE FLOWS IMPULSIVELY STARTED FROM REST

E.A. MOSS and D.F. da SILVA

School of Mechanical Engineering, University of the Witwatersrand
Johannesburg, PO Wits 2050, SOUTH AFRICA

Abstract

The purpose of this study was to compare experimental transition results with analytical predictions of instability in spatially developed pipe flows impulsively accelerated from rest. The base flow environment is a time-dependent one in which velocity profiles evolve from an initially 'top-hat' form towards parabolic for large times. A shear stress probe was used to monitor experimentally the local conditions under which transition occurred. The processed results were compared with stability predictions, using critical Reynolds number versus a dimensionless shear stress parameter. Measured transition was found to *precede* instability. When the results were reprocessed to reflect critical Reynolds number based on displacement thickness versus dimensionless time, the analytical and experimental results appeared to approach approximately the same point for zero time, consistent with the boundary layer limit in the presence of finite amplitude disturbances. A possible explanation for the presence of the disturbances is the upstream travelling turbulent front itself.

Notation

c	Phase velocity
$\overline{c}$	Dimensionless phase velocity $[c/U_0]$
D	Pipe diameter
E	Voltage output of hot wire anemometer
Re	Reynolds number based on diameter $[U_0 D/\nu]$
Re_R	Reynolds number based on radius $[U_0 R/\nu]$
Re_{δ^*}	Reynolds number based on displacement thickness $[U_0\delta^*/\nu]$
r	Radial co-ordinate
$\overline{r}$	Dimensionless radial co-ordinate $[r/R]$
R	Pipe radius
S	Velocity profile shape parameter $[\tau_w d/(\mu U_0)]$
t	Time
$\overline{t}$	Dimensionless time $[\nu t/R^2]$
u	Axial velocity
$\overline{u}$	Dimensionless axial velocity $[u/U_0]$
U	Base flow axial velocity
$\overline{U}$	Dimensionless base flow axial velocity U/U_0
U_0	Pipe cross-sectional mean velocity
Greek	
α	Wavenumber
$\overline{\alpha}$	Dimensionless wavenumber $[\alpha R]$
α^*	Dimensionless wavenumber $[\alpha\delta^*]$
δ	Boundary layer thickness
δ^*	Displacement thickness
ζ	Vorticity
$\overline{\zeta}$	Dimensionless vorticity $[\zeta R/U_0]$
$\overline{\lambda}$	Dimensionless wavelength $[2\pi/\overline{\alpha}]$
ν	Fluid kinematic viscosity
τ_w	Wall shear stress
ϕ	Dimensionless amplitude function
ψ	Stream function
$\overline{\psi}$	Dimensionless stream function $[\psi/(U_0 R^2)]$
ψ'	Dimensionless perturbation of stream function
$\overline{\omega}$	Dimensionless critical frequency $[\alpha^*\overline{c}]$

INTRODUCTION

This analytical and experimental study is concerned with laminar to turbulent transition in spatially fully developed pipe flows impulsively started from rest. In such a system velocity profiles evolve from a 'top-hat' shape at zero time ($t = 0$) towards parabolic as $t \to \infty$. Depending on the Reynolds number, at some intermediate time instability followed by transition may occur.

Study of instability and transition in pipe flows monotonically accelerated from rest appear to have been confined to the largely experimental papers of Kataoka et al (1975), Maruyama et al (1978), van de Sande et al (1980), Moss (1989) and Lefebvre & White (1989). Of these authors only Moss and Lefebvre & White observed *local* transition, rather than turbulent structures *washed down* from the inlet after startup. In fact Moss (1989) observed both modes of transition and accounted for them in a formal way. Nevertheless no work in unsteady (non-pulsatile and non-oscillatory) pipe flows has thusfar produced even qualitative tie-up with analytical stability results.

The objective of this study was to measure the onset of transition in an impulsively started pipe flow, and to represent the results in an appropriate framework in which they might be reconciled with a linear stability analysis.

EXPERIMENTATION

The test rig used in the current investigation comprised a stainless steel pipe, 15.6 mm in diameter, mounted vertically and supplied by a constant head tank. The final Reynolds number Re ($= U_0 D/\nu$) was dictated by the setting of a precision needle valve, whose constriction was high relative to wall friction, thus ensuring constant flow after a quick-acting solenoid valve provided a rapid flow increase from rest. The valves were positioned at the end of the pipe, approximately 1.5 m downstream of a Disa type 55R47 glue-on shear stress probe which was 4.54 m (291 diameters) from the pipe inlet. The working fluid was kerosene. Flow measurement was achieved by an orifice meter located below the test section. A simple inlet contraction was included, which did not prevent the intermittent occurrence of turbulence in the tube at a steady state Re of about 2 400 (effectively a disturbed inlet). The analogue output of the shear stress probe was directed into a Nicolet digital oscilloscope which was triggered by the solenoid valve. Figure 1 shows a typical output from the shear stress probe after a rapidly started flow under a constant head of liquid.

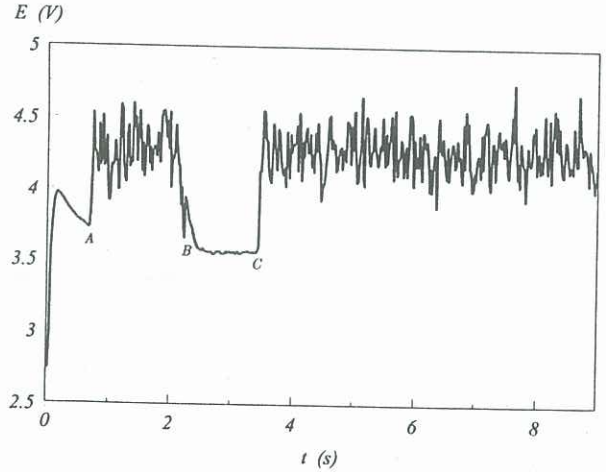

Figure 1. Typical output from shear stress probe.

In Moss (1989) the first laminar to turbulent event (A in figure 1) was interpreted as a 'natural' stable/unstable front moving rapidly up the tube as local conditions become met; the subsequent turbulent to laminar transition (B) was ascribed to the washdown of the first event by the approach of the generated turbulence from upstream - itself seen as a second laminar to turbulent event (C). The shear stress probe was calibrated according to the relationship $E^2 = A + B\tau_w^{1/3}$ (E = voltage; τ_w = shear stress) to establish the laminar conditions existing at A. The cross-sectional mean velocity U_0 at transition was obtained from the flowrate measured using a simple orifice meter.

Transition was found to occur at diminishing times with increasing Reynolds numbers, and for $Re >\simeq 12\,500$ occurred during the flow acceleration.

ANALYSIS

Velocity Profile Shape Parameter

From the outset a suitable parametric framework was required within which the onset of flow instability and transition might be viewed. Appropriate groups were found to be the Reynolds number (Re) and, in view of the fact that a shear stress probe was used in the experimentation, a dimensionless shear stress defined by $S = \tau_w D/(\mu U_0)$, which it may be shown (Moss, 1985) for this class of flows uniquely defines the velocity profile shape at a particular time. A top-hat velocity profile is reflected by $S \rightarrow \infty$ and a parabolic shape for $S = 8$.

Linear Stability

In view of the fact that the flow acceleration was negligible when transition occurred, the following *quasis-steady* approach to the stability problem appears to be justified (Shen, 1961):

The vorticity-stream ($\zeta - \psi$) form of the two-dimensional, incompressible, axisymmetric Navier Stokes equations were non-dimensionlized according to $\overline{r} = r/R$; $\overline{x} = x/(R.Re_R)$; $\overline{t} = (\nu t)/R^2$; $\overline{u} = u/U_0$; $\overline{v} = (vRe_R)/U_0$; $\overline{\psi} = \psi/(U_0 R^2)$ and $\overline{\zeta} = (\zeta R)/U_0$, where ζ is the vorticity and the other symbols have their usual meaning. Provided $Re_R >> 1$ the equations reduce to the following:

$$\frac{\partial\overline{\zeta}}{\partial\overline{t}} + \frac{\partial(\overline{\zeta}\,\overline{v})}{\partial\overline{r}} + \frac{\partial(\overline{\zeta}\,\overline{u})}{\partial x} = \frac{\partial^2\overline{\zeta}}{\partial\overline{x}^2} + \frac{\partial}{\partial\overline{r}}\frac{1}{\overline{r}}\frac{\partial\overline{\zeta r}}{\partial\overline{r}} \qquad (1)$$

$$\begin{aligned} \frac{1}{2\pi\overline{r}}\frac{\partial\overline{\psi}}{\partial\overline{r}} &= \overline{u} \\ -\frac{1}{2\pi\overline{r}}\frac{\partial\overline{\psi}}{\partial\overline{x}} &= \overline{v} \end{aligned} \qquad (2)$$

$$-\overline{\zeta} = \frac{1}{2\pi\overline{r}}\left[\frac{\partial^2\overline{\psi}}{\partial\overline{x}^2} + \frac{\partial^2\overline{\psi}}{\partial\overline{r}^2} - \frac{1}{\overline{r}}\frac{\partial\overline{\psi}}{\partial\overline{r}}\right] \qquad (3)$$

To achieve the base flow for the spatially fully developed case, transverse velocities and derivatives in $\overline{x}$ were ignored. The resultant equations were solved using a simple implicit marching technique, yielding, in addition to variations of $\overline{U}$ with $\overline{r}$, the variations of S with $\overline{t}$ shown in figure 2, commensurate with a velocity profile development from a 'top hat' to a parabolic shape.

The linear stability is required of a parallel axisymmetric base flow having the velocity components

$[\overline{U}(\overline{r},\overline{t}),0,0)]$, which is perturbed by an axisymmetric disturbance with the mathematically convenient form $\psi'(\overline{x},\overline{r},\overline{t}) = \phi(\overline{r})\exp[i\overline{\alpha}(\overline{x}-\overline{c}\overline{t})]$. For the temporal (as opposed to spatial) stability problem under consideration ϕ is a complex amplitude function given by $\phi(\overline{r}) = \phi_r + i\phi_i$ and the dimensionless celerity of disturbance propagation (phase velocity) is defined by $\overline{c} \equiv c/U_0 = \overline{c}_r + i\overline{c}_i$ where $\overline{c}_r$ is the velocity of wave propagation in the base flow direction and $\overline{c}_i$ determines the degree of damping (negative) or amplification (positive). The dimensionless wavenumber $\overline{\alpha}$ ($\equiv \alpha R$) is real and related to the dimensionless wavelength by $\overline{\lambda} = 2\pi/\overline{\alpha}$.

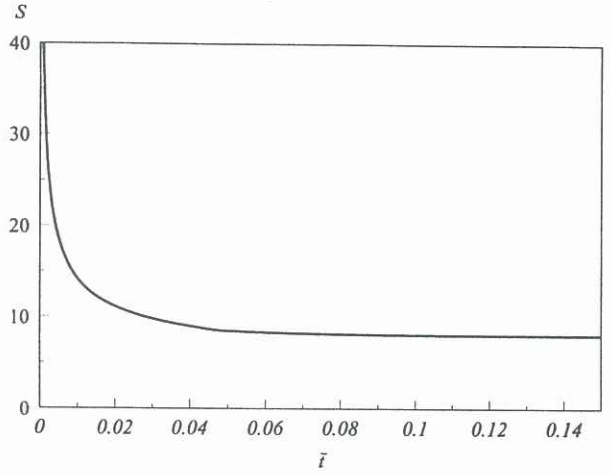

Figure 2. Variation of velocity profile shape parameter with dimensionless time.

Substitution into equations (1) to (3) and linearization leads to the Sexl (1927) equation given by

$$\frac{1}{(i\alpha Re_R)}(L-\overline{\alpha}^2)^2\phi = (\overline{U}-\overline{c})(L-\overline{\alpha}^2)\phi - \overline{r}(\overline{U}'/\overline{r})'\phi \qquad (4)$$

where $\overline{U}' \equiv d\overline{U}/d\overline{r}$ and $L \equiv d^2/d\overline{r}^2 - (1/\overline{r})d/d\overline{r}$.

A singular eigenvalue problem results, requiring that $\phi/\overline{r}$ and $\phi'/\overline{r}$ be bounded as $\overline{r} \longrightarrow 0$. At the rigid boundary ($\overline{r} = 1$) $\phi = \phi' = 0$. This is a characteristic value (eigenvalue) problem of the form $\mathcal{F}(\overline{\alpha},\overline{c},Re_R) = 0$ whose solution entails the determination of the complex celerity $\overline{c}$ (the eigenvalue), for various values of Re_R and $\overline{\alpha}$. Consequently the locus $\overline{c}_i = 0$ may be obtained, defining the curve of neutral stability for a particular velocity profile. The critical Reynolds number of stability is the point on the curve where the Reynolds number has its smallest value.

A finite difference approach was adopted in conjunction with the Q-Z algorithm developed by Moler & Stewart (1973). This technique, chosen because of its efficiency in computing eigenvalues for singular matrices, is more fully described in da Silva & Moss (1988). Predictions are shown in Table I, together with computations of Reynolds number based on displacement thickness, obtained from the product of Re and δ^*/D.

Table I. Flow and stability data for the current investigation.

S	Re_R	$\overline{c} = \overline{c}_r$	$\overline{\omega}$	U_c/U_0	Re_{δ^*}
54.74	23450	0.4176	0.11967	1.046	525.5
45.77	19750	0.4221	0.11717	1.056	533.2
40.50	17800	0.4242	0.11439	1.065	548.3
36.92	16550	0.4256	0.11164	1.072	563.9
32.23	14940	0.4285	0.10854	1.085	591.3
28.05	13550	0.4322	0.10417	1.101	626.8
25.41	12680	0.4358	0.10066	1.115	656.7
23.04	11910	0.4408	0.09717	1.131	690.9
21.74	11530	0.4441	0.09434	1.141	715.9
18.92	10870	0.4560	0.08723	1.172	797.0
17.26	10990	0.4663	0.07976	1.197	903.9
16.10	12180	0.4720	0.06988	1.220	1092.9
15.23	13930	0.4793	0.06042	1.240	1340.4
14.55	18140	0.4846	0.04644	1.258	1849.1
14.00	19700	0.4835	0.02280	1.275	4223.0

RESULTS & DISCUSSION

Figure 3 shows the variation of critical Reynolds number (Re) with velocity profile shape parameter (S). Both experimental transition results and computed stability data are represented on the same axes. Beyond a Reynolds number of approximately 12 500 transition occurred during the flow acceleration: therefore the experimental results were disregarded for comparison purposes beyond that point. Consistent with steady pipe entrance flows the stability analysis indicates that the limits corresponding to top-hat and parabolic velocity profiles are stable at all Reynolds numbers to infinitesimal disturbances. It is apparent that a rather poor correlation occurs between theory and analysis, apparently diminishing with increasing values of S; in particular the onset of instabilities would be expected to *precede* transition; whereas in this case transition occurs at a lower Reynolds number than predicted by stability analysis - an indication of so-called 'sub-critical' transition.

In order to explore the apparent asymptotic tendency of the results in the limit $\overline{t} \rightarrow 0$, they were reprocessed to yield a plot of critical Reynolds number based on displacement thickness vs dimensionless time (figure 4). It may be seen that the theoretical results tend towards the classical parallel, zero pressure gradient boundary layer limit of Jordinson (1970). This is a not unexpected result in view of the fact that $\delta \rightarrow 0$ as $\overline{t} \rightarrow 0$, i.e. for small values of time δ/R is small. It is noted that the experimental data also appears to approach approximately the same limit. Outside of possible correlation towards this limiting value, the anomaly between measured and predicted results is not dissimilar to the very poor comparison between Sarpkaya's (1975) experimental measurements of pipe flow entrance stability, and entrance flow stability predictions.

The above behaviour of the experimental system suggests that the conditions pertaining to the

measured and predicted data were different. In the probable absence of non-parallel effects the most likely cause of this appears to have been the presence of finite amplitude disturbances in the system. Speculation then arises as to their possible origin, because local transition was generally observed a substantial period of time before the arrival of the inlet generated turbulence from upstream: therefore it is unlikely that this was a contributory factor. A possible explanation is as follows: as the turbulent interface moves *upstream* its presence effectively subjects successive sites to large-amplitude broad-band noise. Thus the instability/transition events occur in an environment of finite disturbances, rather than that of infinitesimal magnitude assumed for the stability analysis. In a similar context propagation of turbulence by destabilization is an accepted hypothesis (for example Glezer et al, 1989), but it has previously hitherto been applied to the advection of turbulence in a *downstream* direction.

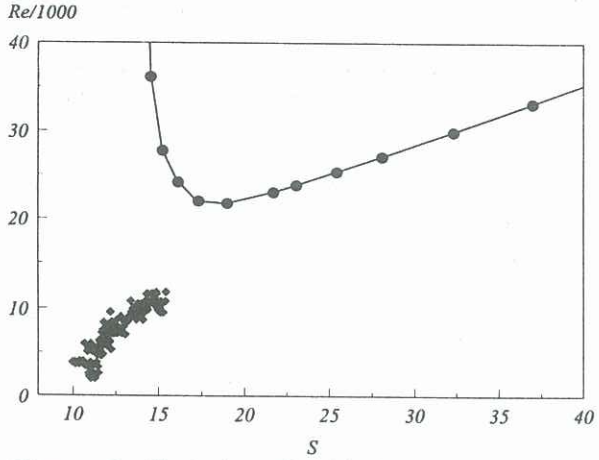

Figure 3. Variation of critical Reynolds number with velocity profile shape parameter; ●: stability predictions; ◆: transition measurements.

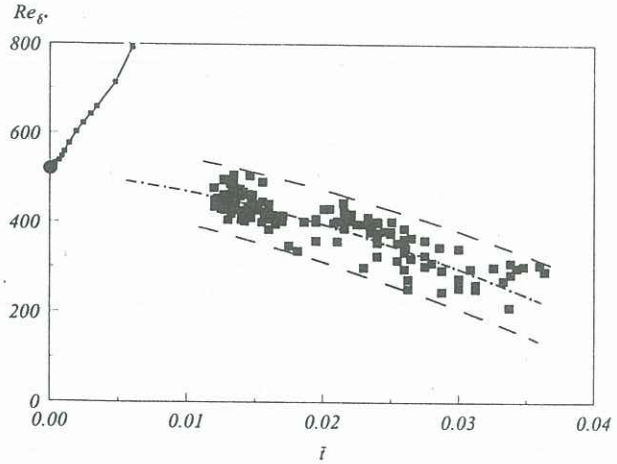

Figure 4. Variation of critical Reynolds number based on displacement thickness with dimensionless time; ▪: stability predictions; ■: transition measurements; ●: boundary layer prediction of Jordinson (1970).

For cases where δ/R is not small little appears to be known in the literature regarding the effect of finite disturbances on stability and the advent of transition. However the apparent convergence of analysis and theory as $\bar{t} \rightarrow 0$ (and hence $\delta/R \rightarrow 0$) may be explained by the well-established evidence in the literature (for example Granville, 1953) that for boundary layers as the level of turbulence intensity increases the momentum thickness (and hence displacement thickness) Reynolds numbers for predicted instability and measured transition approach each other.

In conclusion: although more detailed experimental work is required, particularly to characterize the nature of the upstream-moving turbulent front and its possible influence on local instability and transition, (i) an appropriate framework has been developed for comparing analsysis with experimentation, and (ii) some insights have been gained into the effects of finite disturbances on unsteady pipe flows.

REFERENCES

GLEZER A, KATZ Y & WYGNANSKI I (1989) *On the breakdown of the wave packet trailing a turbulent spot in a laminar boundary layer.* J. Fluid. Mech., 198, 1-26.

GRANVILLE P S (1953) *The calculation of viscous drag of bodies of revolution.* Navy Dept. The David Taylor Model Basin; Rep. 849.

JORDINSON R (1970) *The flat plate boundary layer. Part 1. Numerical Integration of the Orr-Sommerfeld equation.* J. Fluid. Mech., 43, pt 4, 801-811.

KATAOKA K, KAWABATA T & MIKI K (1975) *The start-up response of pipe flow to a step change in flow rate.* J. of Chem. Eng. of Japan, 8, n4, 266-271.

LEFEBVRE P J & WHITE F M (1989) *Experiments on transition to turbulence in a constant acceleration pipe flow.* Trans ASME, 111, 428-432.

MARUYAMA T, KATO Y & MIZUSHINA T (1978) *Transition to turbulence in starting pipe flows.* J.of Chem. Eng. of Japan, 11, n5, 346-353.

MOSS E A (1985) *PhD Thesis* University of the Witwatersrand, Johannesburg.

MOSS E A (1989) *The identification of two distinct laminar to turbulence transition modes in pipe flows accelerated from rest.* Experiments in Fluids, 7, 271-274.

SHEN S F (1961) *Some considerations on the laminar stability of time-dependent flows.* Jnl. of Aero. Sci., 28, 397-404.

VAN DE SANDE E, BELDE A P, HAMER B J G & HIEMSTRA W (1980) *Velocity profiles in accelerating pipe flows started from rest.* BHRA 3rd Int. Conf. on Pressure Surges, 1-14.